

Optical Performance Monitoring in High-speed Optical Fiber Communication Systems

Changyuan Yu^{*a,b}, Jing Yang^a, Junhao Hu^a, and Banghong Zhang^a

^aDept. of Electrical & Computer Engineering, National University of Singapore, Singapore, 117576;

^bA*STAR Institute for Infocomm Research (I2R), Singapore, 138632

ABSTRACT

Optical performance monitoring (OPM) becomes an attractive topic as the rapid growth of data rate in optical communication networks. It provides improved operation of the high capacity optical transmission systems. Among the various impairments, chromatic dispersion (CD) is one of major factors limiting the transmission distance in high-speed communication systems. Polarization-mode dispersion (PMD) also becomes a degrading effect in the system with data rate larger than 40 Gbit/s. In this paper, we summarize several CD and PMD monitoring methods based on RF spectrum analysis and delay-tap sampling. By using a narrow band fiber Bragg grating (FBG) notch filter, centered at 10 GHz away from the optical carrier, 10-GHz RF power can be used as a CD-insensitive PMD monitoring signal. By taking the 10-GHz RF power ratio of non-filtered and filtered signal, PMD-insensitive CD monitoring can be achieved. If the FBG notch filter is placed at optical carrier, the RF clock power ratio between non-filtered and filtered signal is also a PMD-insensitive CD monitoring parameter, which has larger RF power dynamic range and better measurement resolution. Both simulation and experiment results show that the proposed methods are efficient on measuring CD and PMD values in 57-Gbit/s D8PSK systems. Delay-tap sampling is another efficient method of measuring residual CD. Amplitude ratio of asynchronous delay-tap sampling plot decreases with CD monotonously, and the amplitude ratio can be obtained by using low bandwidth balanced receiver. The simulated results show that our method is efficient on residual CD measurement in 50-Gbit/s 50% RZ DQPSK systems with a 12-GHz balanced receiver. Since no modification on the transmitter or receiver is required, the proposed scheme is simple and cost effective.

Keywords: Chromatic dispersion (CD), fiber Bragg grating (FBG), optical communications, optical performance monitoring (OPM), polarization-mode dispersion (PMD)

1. INTRODUCTION

Optical performance monitoring (OPM) becomes an attractive topic as the rapid growth of data rate in optical communication networks. It provides improved operation of the high capacity optical transmission systems. Among the various impairments, chromatic dispersion (CD) is one of major factors limiting the transmission distance in high-speed dense wavelength division multiplexing (DWDM) systems. It may change with network reconfigurations and many environmental conditions such as temperature. Hence, real-time CD monitoring has attracted a lot of interests. The pilot tone method [1, 2] was proposed to monitor CD value by measuring phase difference between the upper and lower sidebands of the subcarrier signal. However, the pilot tone could interfere with data and cause power penalty in the system. CD induced radio-frequency (RF) clock fading was proposed to monitor CD for return-to-zero (RZ) and non-return-to-zero (NRZ) signals [3, 4]. However, the measurement results are affected by the polarization mode dispersion (PMD) effect. Another method based on power ratio of two RF tone powers was proposed in [5]. It requires modification of the transmitter, and the added RF tones may introduce degradation on data quality. Eye diagrams have been considered as a useful tool for monitoring CD, PMD, signal-to-noise ratio (SNR) and other impairments in optical transmission systems [6]. However, clock synchronization is required so that the sampling can be synchronized to the signal. Many monitoring techniques have been proposed based on asynchronous sampling method [7-9], which can operate without clock extraction. However, it is still challenge to identify a particular impairment in the present of other impairments. Recently, asynchronous delay-tap sampling was reported [10, 11]. This method uses a delay-tap line and a pair of data could be obtained in one sampling. Multiple impairment measurements as well as signal quality are extracted from the two dimensional histogram of signal. CD monitoring for differential phase shift keying (DPSK) signal by utilizing asynchronous delay-tap sampling was proposed, while a phase shift of $\pi/4$ should be added in one arm of conventional DPSK receiver [12]. Asymmetry ratio of delay-tap sampling is proposed on residual CD monitoring for

differential quadrature phase shift keying (DQPSK) signal [13]. However, for the reported asynchronous delay-tap sampling methods, the measurement resolution is not high when the residual CD is small.

PMD becomes a degrading effect in high-speed, long haul optical fiber transmission systems. Various methods have been reported to monitor and compensate PMD in the optical network systems. One method is measuring the difference between the two optical frequency components for the two orthogonal principal states of polarization (PSPs) [14]. However, polarization tracking is required in the system. Another method was reported to measure the differential group delay (DGD) by monitoring the degree-of-polarization (DOP) of received signal [15, 16]. This method depends on the pulse width of the signal and the DGD monitoring range is small for short pulses. RF tone power can be used to monitor PMD, but the effects of CD on RF tone may introduce measurement errors [17, 18]. Eye diagrams and delay-tap plots reveal the effect of PMD [19, 20], while it is still challenging to measure the value of PMD in the presence of other impairments.

In this paper, we summarize several CD and PMD monitoring methods based on RF spectrum analysis and delay-tap sampling plot in high-speed transmission systems ($> 40\text{Gbit/s}$). In method 1, by using a fiber Bragg grating (FBG) notch filter centered at 10 GHz away from the optical carrier, PMD value can be measured by 10 GHz RF power of filtered branch [21-23] and CD value can be monitored by 10GHz RF power ratio [24]. In method 2, a narrow band FBG filter is centered at optical carrier wavelength, and the RF clock power ratio can be used as a PMD-insensitive CD monitoring signal, which has larger dynamic range compared with method 1[25]. Once CD value is determined, DGD value can be traced by RF clock power in the branch without filtering. However, CD and PMD measurement ranges are limited compared with that of method 1. Both simulation and experiment results show that the proposed methods are efficient on measuring CD and PMD values in 57-Gbit/s differential 8-level phase-shift keying (D8PSK) systems. In method 3, amplitude ratio of asynchronous delay-tap sampling is used as CD monitoring signal. By using a balanced receiver with a bandwidth of 12-GHz, the CD measurement range is increased in a 50-Gbit/s RZ-DQPSK system.

2. PERFORMANCE MONITORING BASED ON RF SPECTRUM ANALYSIS

The principle of PMD and CD effects on RF power of NRZ signal is shown in Fig.1. Chromatic dispersion through the fiber link changes the phase of the sidebands compared with the carrier, and the RF clock power increase with CD. First-order PMD effect, DGD, changes the phase difference of signal at two PSPs. If DGD value equals to half period time of a certain frequency, the optical components at the two orthogonal polarization states have a phase shift of π and there is no beating component at corresponding RF frequency. For NRZ signal, RF power increases with CD and decreases with DGD. If one sideband is filtered out, CD results in phase shift to the RF tone while the amplitude of RF tone keeps constant. PMD induces RF tone power fading and the fading effect is the same regardless of whether the notch filter is present or not. Therefore, CD-insensitive PMD measurement can be achieved by monitoring the RF tone power of filtered signal. PMD-insensitive CD values can be measured by using the RF tone power ratio of the non-filtered and filtered signal. The frequency of RF tone determines the measurement range and sensitivity. We introduce two CD and PMD monitoring methods based on RF spectrum analysis. In method 1, a narrow band FBG notch filter is placed at 10-GHz away from the carrier in a 57-Gbit/s D8PSK systems. The 10-GHz RF tone power keeps constant as CD increases and decreases as PMD increases, which is a CD-insensitive PMD monitoring signal. By taking the 10-GHz RF power ratio of non-filtered and filtered signal, PMD effects on RF power can be eliminated and PMD-insensitive CD measurement can be achieved. Compared with the method using RF clock tone as monitoring signal, the CD measurement range is increased and the required bandwidth of the photodetector is lower.

In method 2, the optical carrier is filtered out by a narrow band FBG filter, and the RF clock power can be regenerated in back-to-back case. The reason is that the carrier as well as the optical components around carrier is filtered out by FBG. The components around carrier are related to the low RF frequency tones, which have long period in time domain. Therefore, the waveform at clock frequency is dominant by filtering out these components. After propagation through fiber link, the accumulated CD induces distortion on the signals. For the NRZ signal filtered by FBG, the RF clock power decreases with CD, which is opposite to that without filter. Therefore, the RF power ratio between the non-filtered and filtered signal increases with CD and has large dynamic range, which results in better measurement resolution compared with method 1. On the other hand, PMD induces RF tone power fading through the transmission and the fading effect is the same regardless the notch filter is present or not. By taking the RF clock power ratio of non-filtered and filtered signal, PMD effects on RF clock power can be eliminated. Compared with method 1, measurement resolution is improved; while, the CD measurement range is decreased from 500ps/nm to 200ps/nm. Once CD value is determined, DGD value can be traced by RF clock power in the branch without filtering.

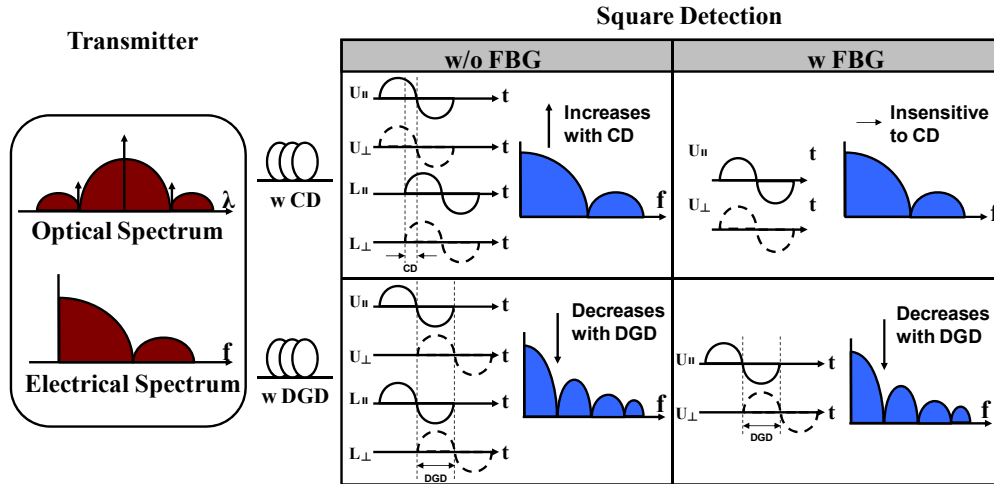


Figure 1. Principle of PMD and CD effects on the RF power of NRZ signal. U_{ii} (L_{ii}): signal of one PSP in upper (lower) sideband; U_{\perp} (L_{\perp}): signal of the other PSP in upper (lower) sideband.

Fig. 2 shows the experimental setup of CD monitoring scheme in a NRZ D8PSK system based on RF spectrum analysis. 57-Gbit/s D8PSK signal was generated by using one in-phase/quadrature (I/Q) modulator and one phase modulator (PM). Several spans of dispersion compensation fiber (DCF) were used to provide different CD values. First-order PMD was emulated by utilizing two polarization beam splitters (PBSs) and a tuneable optical delay line. At one of monitoring branch, an FBG notch filter with bandwidth of 0.06 nm and reflection of 15 dB is used to filter out part of optical component. The other monitoring branch is detected by a photodetector directly. RF spectrum analyzers are used to monitoring the RF power at various frequencies. The RF spectrum analyzers can be replaced by electrical bandpass filters and power meters, which are more cost effective.

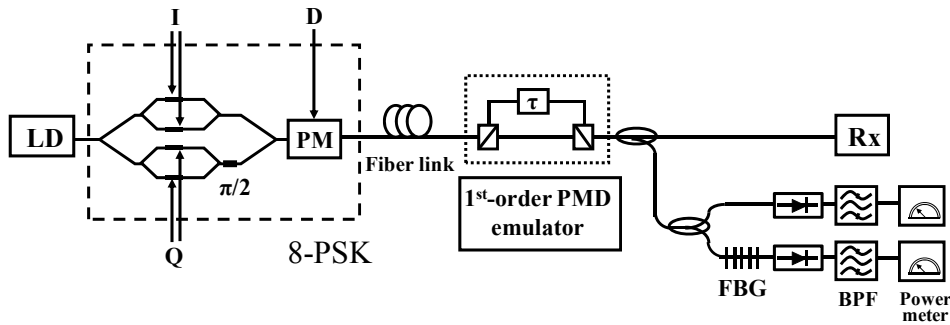


Figure 2. System setup of CD and PMD monitoring utilizing FBG notch filter in D8PSK system. PM: phase modulator; Rx: receiver; BPF: bandpass filter.

2.1 PMD and CD Monitoring by Placing FBG filter at 10GHz Away From Carrier

CD-insensitive PMD measurement can be realized by placing a FBG filter at 10GHz away from the carrier and monitoring the 10GHz RF tone power. Fig. 3(a) shows the measured optical spectrum (with resolution of 0.01nm) of a 57-Gbit/s D8PSK signal filtered by a narrow band FBG notch filter (with bandwidth of 0.06 nm and reflection of 15 dB). The optical component at 10 GHz away from the carrier was filtered out; therefore, the 10 GHz RF tone power is equivalent to that of single sideband (SSB) signal detected by photodetector (PD). Fig. 3(b) shows the 10 GHz RF tone power as a function of DGD in 57-Gbit/s D8PSK system. The power splitting ratio between the two principle-polarization-states is 0.5. Different CD values (0, -166 and -330-ps/nm) were introduced by several spans of DCF. The intensity of 10 GHz RF tone reaches its minimum value when the DGD equals to 50-ps. This is due to the fact that the 10GHz components of the two orthogonally polarized signals have a phase shift of π and hence cancel out each other under DGD of 50-ps. The 10-GHz RF power varies as a function of DGD and the measurement range is increased to 50 ps, while it is only 26.3 ps if one of optical clocks is filtered out and 19-GHz RF tone is used as monitoring signal. It is

observed that the 10-GHz RF tone power is not affected by CD values. The FBG notch filter can be placed closer to the carrier, and the DGD measurement range will be increased further. However, the bandwidth of the FBG should be much narrower to avoid the filtering of carrier.

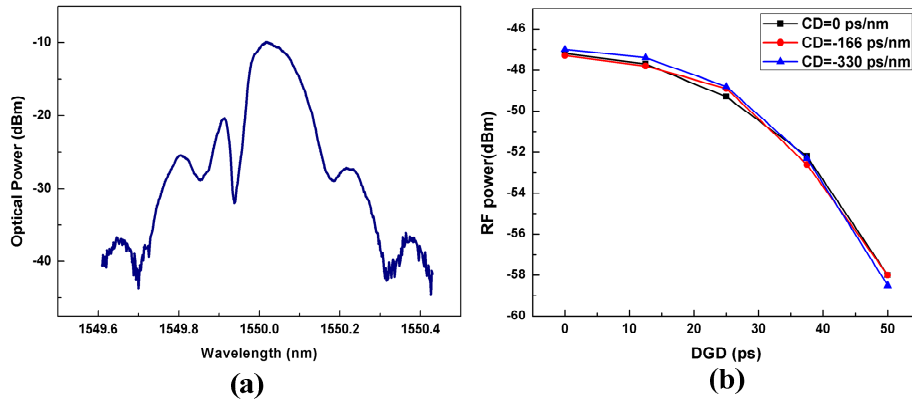


Figure 3. (a) Optical spectrum of a 57-Gbit/s D8PSK signal filtered by an FBG notch filter placed at 10-GHz away from the carrier wavelength; (b) RF power at 10-GHz as a function of DGD for different CD values for a 57-Gbit/s D8PSK system.

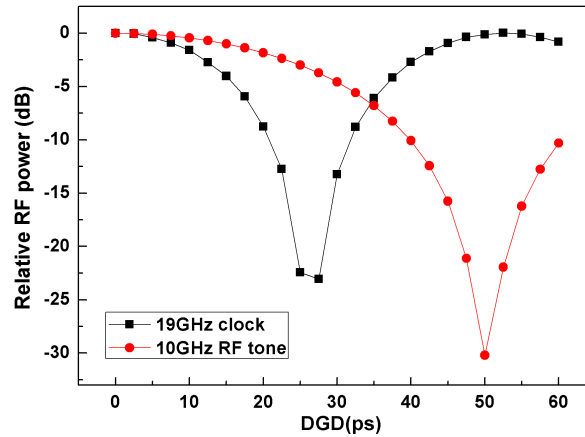


Figure 4. Relative RF powers as a function of DGD for 38-Gbit/s DQPSK signal when 10-GHz RF tone and 19-GHz clock are monitoring signals.

The numerical simulation is calculated in the simulation tool VPItransmission 7.0. Fig. 4 shows the simulation results of relative 19 GHz RF clock and 10 GHz RF tone power as a function of DGD in 38-Gbit/s DQPSK system. The power splitting ratio between the two principle-polarization-states is 0.5. An FBG notch filter (with a rejection of 15 dB and 3 dB bandwidth of 0.06 nm) was centered at clock and 10 GHz away from the carrier, respectively. The DGD measurement range is only 0~26.3 ps when the FBG filter is centered at one of optical clock and 19-GHz RF clock is used as monitoring signal, while the DGD measurement range is increased to 0~50 ps by using the 10-GHz RF tone as a monitoring signal. In the proposed method, the DGD measurement range is increased; however, the accuracy of DGD measurement decreases, especially in the small DGD region. There is a trade-off between resolution and measurement range when RF tone is utilized as monitoring signal.

Fig. 5(a) shows the effects of optical signal-to-noise ratio (OSNR) on the PMD measurement results. It is observed that the dynamic range of RF power increases with OSNR. This is because the 10-GHz RF power reaches its minimum value when DGD equals to $(NT+1)/2$. T is period time of 10 GHz RF tone and N is an integer. In these cases, the noise power is comparable to the 10-GHz RF power, and the measurement results are affected much by the noise. Therefore, the OSNR affects the measurement results when RF power is small, where DGD is close to 50 ps. If the OSNR is less than 20 dB, the detected RF power has fluctuations and calibration is required.

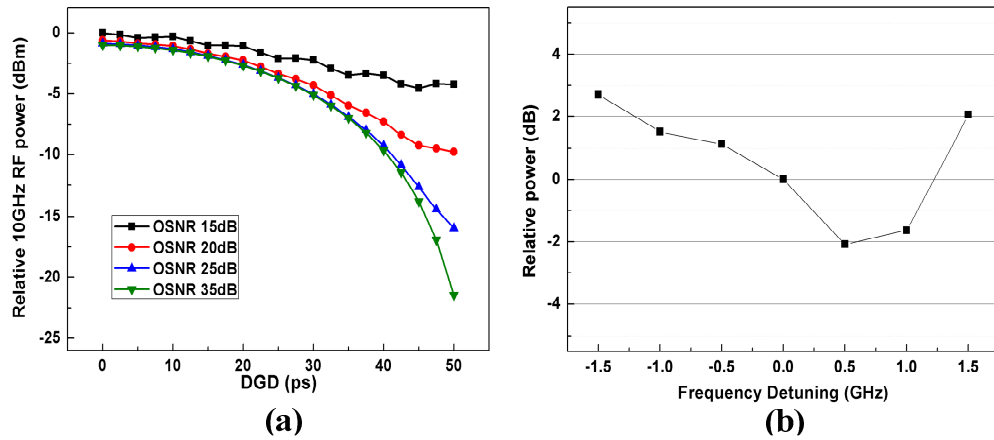


Figure 5. (a) OSNR effects on the DGD measurement results; and (b) relative 10-GHz RF power as a function of DGD under FBG filter frequency detuning in 38-Gbit/s DQPSK system.

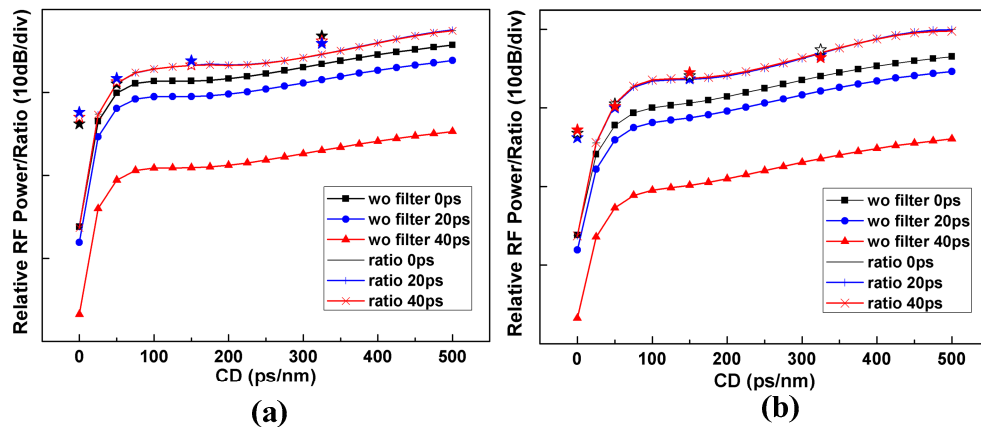


Figure 6. Relative 10-GHz RF power/ratio as function of CD for (a) 57-Gbit/s D8PSK signal; (b) 38-Gbit/s DQPSK signal (lines for simulation; stars for experiment).

The center wavelength of FBG filter may shift from the original value under various environment effects, which may introduce RF power fluctuations and measurement errors. Fig. 5(b) shows the effects of FBG frequency detuning on the 10GHz RF power in 38-Gbit/s DQPSK system. The 10-GHz RF power change is less than 2 dB when the FBG frequency detuning is smaller than 1 GHz.

As PMD induced RF tone power fading is the same regardless the notch filter is present or not, the 10-GHz RF power ratio of the non-filtered and filtered signal can be used on PMD-insensitive CD monitoring. Fig. 6(a) shows simulation and experimental results of 10GHz RF tone power and power ratio as a function of CD in 57-Gb/s NRZ-D8PSK system. Several DGD values (0, 20 and 40 ps) were introduced by a first-order PMD emulator. It is observed that DGD affects the RF tone power much at absent of FBG filter, which may result in CD measurement errors. If one of the sidebands is filtered out, the DGD effect can be eliminated and accurate CD monitoring can be achieved.

The proposed CD monitoring method is applicable on other modulation formats such as OOK and NRZ-DQPSK. Fig. 6(b) shows the simulation and experimental results of the 10-GHz RF tone power and power ratio versus CD in NRZ-DQPSK transmission system. It is observed that the RF power ratio increases with CD and is almost not affected by PMD effects. Compared with that using 19-GHz RF clock as monitoring signal, the CD measurement range is increased by 3.6 times and the required bandwidth of the photodetector is much lower. Moreover, as the power ratio is used as monitoring signal, the measurement results are independent on the optical power of received signal. It is noted that the monitoring branch, which is filtered by FBG, can be used to achieve CD-insensitive PMD monitoring. Therefore, CD and PMD can be measured simultaneously and independently using our proposed method.

2.2 CD Monitoring by Filtering out Optical Carrier

It is found that the RF clock power of NRZ signal decreases with CD if the optical carrier component is filtered out. On the other hand, the RF clock power increases with CD in the absence of filter. In both cases, RF clock tone power decreases with PMD. Therefore, by taking the ratio of RF clock tone power in the two cases, PMD-insensitive CD measurement can be achieved. Besides, the dynamic range of RF power is improved, which result in better measurement resolution. Fig. 7(a) shows the optical spectrum of 38-Gbit/s DQPSK signal, whose carrier is filtered out by an FBG notch filter. The FBG notch filter has a bandwidth of 0.06 nm and a reflection of 20 dB. The filtering induces distortion to the original signal. By choosing an FBG with suitable bandwidth and reflection, the RF clock tone can be regenerated in the back-to-back case and decreases with CD when transmitting through fiber links and optical components. Fig. 7(b) shows experimental results of relative RF clock tone power as a function of CD in 38-Gbit/s NRZ-DQPSK system in the absence of filter as well as under FBG filtering. Different DGD values (0, 10 and 20 ps) were introduced by a first-order PMD emulator. When there is no filtering, RF clock power increases with CD, which is due to the chromatic dispersion induces phase difference between the sidebands and the beating term is regenerated. It is observed that DGD affects the clock tone power and may introduce errors on CD measurement. When the signal is filtered by an FBG notch filter placed at the carrier wavelength, the received clock power decreases with both CD and DGD values. It is noted that the PMD-induced RF power fading for the filtered and non-filtered signals are the same. Therefore, by taking the power ratio of the two RF clocks, the DGD effects can be eliminated. Fig. 7(c) shows the RF clock tone power ratio of non-filtered and filtered NRZ-DQPSK signal as a function of CD under different DGD values. The RF clock power ratio increases with CD and is almost not affected by DGD. Compared with the methods using RF clock tone as monitoring signal, PMD effect is eliminated and measurement sensitivity is improved. Measurement sensitivity is calculated as the dynamic range of RF power ratio over CD measurement range. Moreover, as the ratio of RF power is used as monitoring signal, the measurement results are not affected by fluctuation of received optical power. However, if the signal power is decreased to a small value (e.g., -20 dBm), the dynamic range of RF power ratio will be limited by the sensitivity of power meter. Fig. 7(d) shows simulated RF power ratio as a function of CD under different optical signal-to-noise ratio (OSNR) levels in 38-Gbit/s DQPSK system. It is observed that OSNR level does not affect the measurement results as long as the signal OSNR is larger than 15 dB.

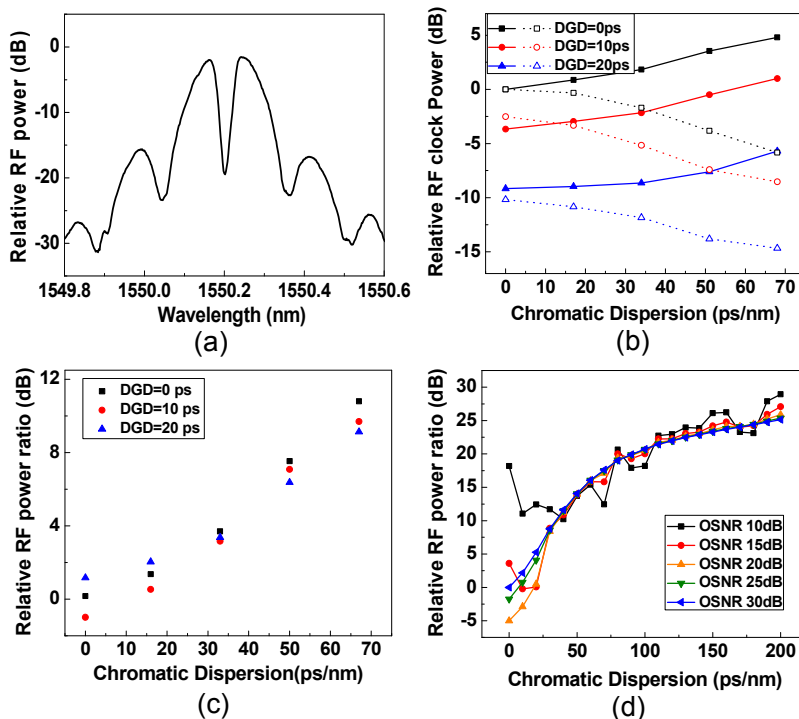


Figure 7. (a) Optical spectrum of DQPSK signal filtered by FBG filter placed at optical carrier wavelength; RF clock power as a function of CD (b) relative RF clock power as a function of CD without filter (solid lines) and with filter (dash lines) under different DGD values; (c) relative RF clock power ratio as a function of CD under different DGD values; (d) simulation of OSNR on measurement results. 38-Gbit/s DQPSK system.

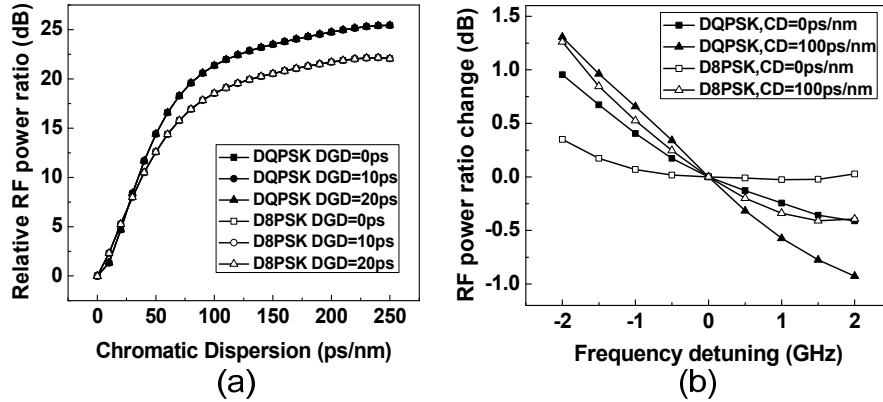


Figure 8. (a) RF clock power ratio change as a function of frequency detuning of FBG filter centered on the optical carrier; (b) RF clock power ratio as a function of CD under different OSNR values.

Fig. 8(a) shows simulation results of RF clock power ratio as a function of CD under different DGD values in 38-Gbit/s NRZ-DQPSK and 57-Gbit/s NRZ-D8PSK systems. It is observed that the CD monitoring range is 0~250 ps/nm in both systems. Besides, DGD does not affect the amplitude of RF power ratio, and the curves under different DGDs (0, 10, and 20 ps) are merged together. In the monitoring window, a dynamic range of more than 20 dB and average sensitivity of >0.1 dB/(ps/nm) can be achieved. The center wavelength of FBG filter may shift from the original value under various environment effects, which may induce RF power ratio changes and CD measurement errors in monitoring scheme. Fig.8 (b) shows the simulated RF clock power ratio change as a function of FBG frequency detuning. CD values may affect RF power ratio fluctuations due to FBG frequency detuning. However, RF clock power ratio change is less than 1.6 dB when the frequency detuning in the range of -2 GHz~2 GHz. If the frequency detuning is less than 1 GHz, the power ratio change is smaller than 0.9 dB.

In proposed method, RF power ratio of two branches is used to eliminate DGD effect. Once CD value is determined, DGD value can be traced by RF clock power in the branch without filtering. However, the absolute RF clock power is affected by received optical power. Fluctuation of optical power will induce DGD measurement errors.

3. CHROMATIC DISPERSION MONITORING BASED ON DELAY-TAP SAMPLING

Asynchronous delay-tap sampling is a technique that provides the information of waveform. Compared with eye diagram, which also express the waveform information of signals, delay-tap sampling has two advantages, which are low sampling rate and no synchronization requirement. Fig. 9(a) shows the schematic graph for generating delay-tap sampling pairs in a demodulated RZ-DQPSK signal. Each point in the delay-tap sampling plot comprises two parameters (x and y). The time delay between x and y is a constant, Δt . It is found that the sensitivities of impairments are different when time delay is changed. The sampling time, T_s , can be many orders of bit period. Therefore, the sampling rate is decreased dramatically and the CD monitoring scheme will be simple and cost effective. Fig. 9(b) shows the demodulated eye diagram of 50% RZ DQPSK signal. Fig. 9(c) shows the asynchronous delay-tap sampling plot at a time delay of half symbol period ($B/2$). Both graphs are in back-to-back case and no distortion is induced.

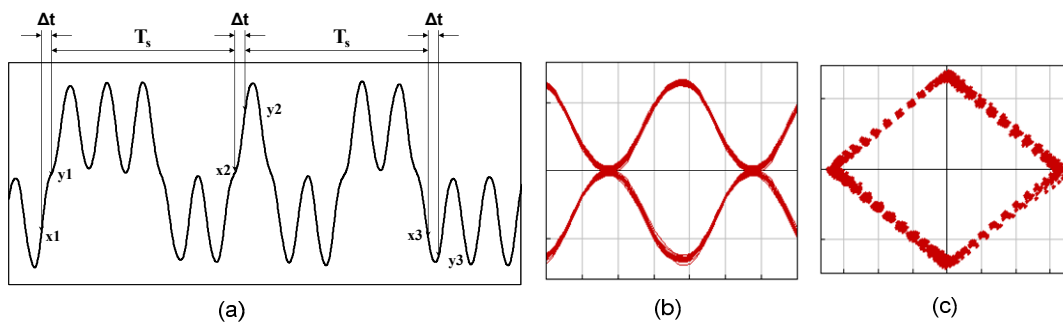


Figure 9. (a) RF clock power ratio change as a function of frequency detuning of FBG filter centered on the optical carrier; (b) RF clock power ratio as a function of CD under different OSNR values.

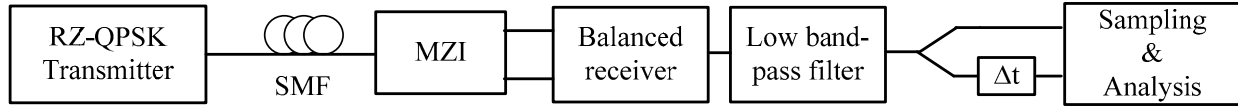


Figure 10. System setup of CD monitoring scheme of 50-Gbit/s RZ-QPSK signal.

In this section, a low bandwidth balanced receiver (12 GHz) is used to detect the signal and obtain the delay-tap sampling plot in a 50-Gbit/s RZ DQPSK system. The simulation results show that CD measurement range is increased and the residual CD can be measured accurately by proposed technique. The system setup of residual CD monitoring in a 50-Gbit/s RZ DQPSK system is shown in Fig. 10. Several pieces of single mode fibers (SMFs) introduce different values of CD. Mach-Zehnder interferometer and balanced receiver are used to demodulate the signal. After that a low bandpass filter, with a 3-dB bandwidth of 12 GHz, is applied to realize our proposed method: using balanced receiver with low bandwidth to plot delay-tap sampling plot and measure the residual CD values in the system with high bit-rate. The shape of the band-pass filter is 4th order Bessel function. The detected electrical signal is split into two branches, while one branch has a time delay (half of the symbol period time, which is 20 ps in 50-Gbit/s DQPSK system) with the other. The obtained sample pairs are delay-tap sampling signals, which reflect the waveform information signal and the distortions induced by various impairments along transmission.

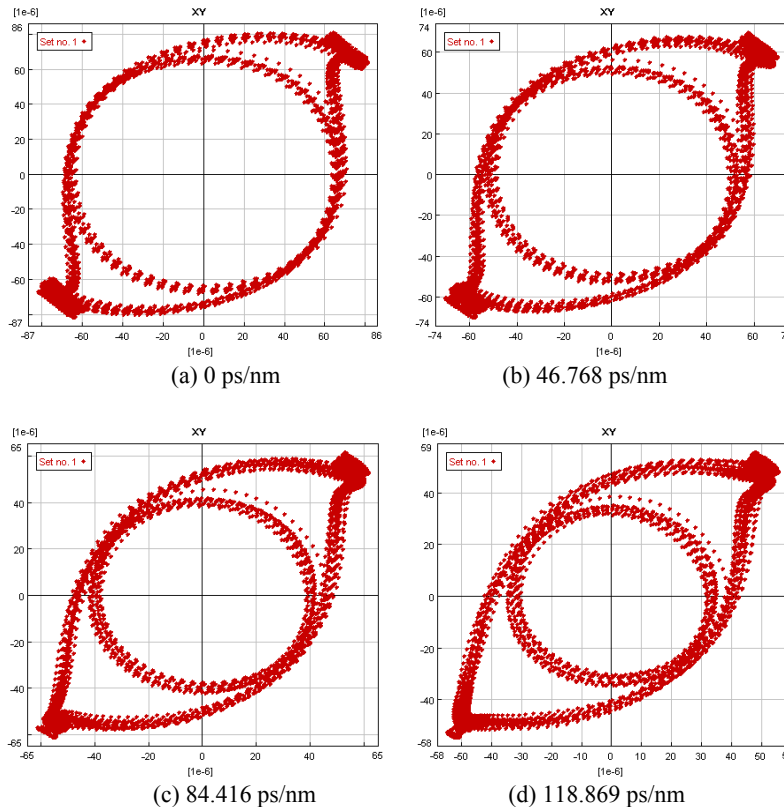


Figure 11. System setup of CD monitoring scheme of 50-Gbit/s RZ-QPSK signal.

Fig. 11 shows the delay-tap sampling plot of demodulated RZ-QPSK signal under different dispersion values, 0-ps/nm, 46.768-ps/nm, 84.416-ps/nm, and 118.869-ps/nm. It is found that the plot is symmetric to the line $y=x$ and $y=-x$, when there is residual dispersion. Moreover, the radius ratio of the outer ring to the inner ring increases monotonously as the increase of the residual CD. Therefore, the radius ratio can be used as a CD monitoring signal. In order to quantify the relationship of this amplitude ratio to the residual CD, amplitude ratio is defined in the delay tap plot.

Fig. 12(a) shows the definition of amplitude ratio. The radius of the inner ring along the line $y = x$ is L_1 , and the radius of the outer ring along $y=-x$ is L_2 . The amplitude ratio of delay tap plot can be defined as:

$$\text{Amplitude ratio} = L_2/L_1 \quad (1)$$

As amplitude ratio is the CD monitoring signal, the measurement results are not affected by received optical power. As shown in Fig. 12(b), the amplitude ratio of delay-tap plot ranges from 0.4 to 0.62 as the residual CD changes from 0-ps/nm to 120-ps/nm. By using a balanced receiver followed by a 12-GHz low band-pass filter, CD measurement range is extended to 130-ps/nm in a 50% RZ DQPSK system. Besides, the residual CD values in the low CD region can also be measured accurately by using this scheme. In the practical systems, the receiver followed by a low band-pass filter can be replaced by a balanced receiver with bandwidth of 12-GHz. Therefore, large CD measurement range can be achieved by using the cost effective low bandwidth balanced receiver in our proposed method.

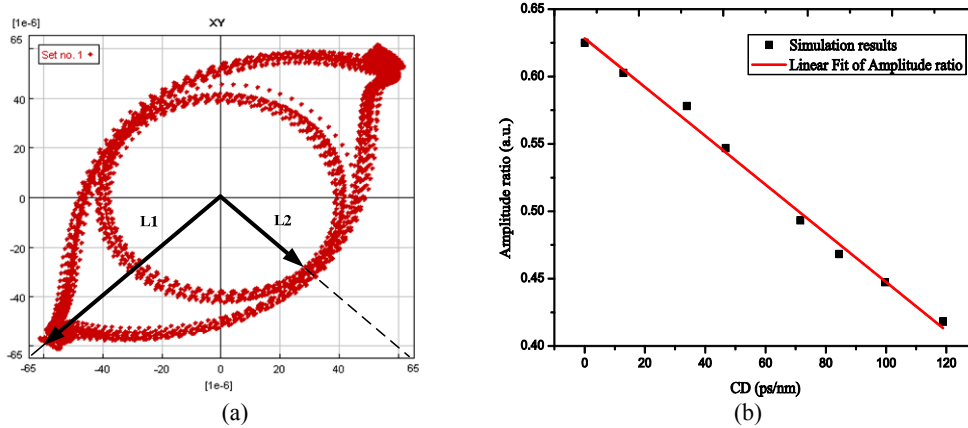


Figure 12. (a) Define amplitude ratio in delay-tap sampling plot; (b) amplitude ratio as a function of residual CD.

4. CONCLUSIONS

CD and PMD monitoring techniques based on RF spectrum analysis with FBG filtering and delay-tap sampling plot are presented. By placing an FBG filter at 10GHz away from the carrier, CD and PMD measurement can be achieved simultaneously. It is shown that the DGD measurement results are not affected by CD and the measurement range is increased to 50-ps in systems with a symbol rate of 19-GSym/s. The CD measurement range is increased to 500ps/nm. Besides, cost effective low-bandwidth photodetector (10GHz) is used in proposed PMD monitoring method. By placing an FBG filter at the carrier wavelength, PMD-insensitive CD measurement with a monitoring range of 0~200-ps/nm, and a dynamic range of more than 25dB can be achieved. Compared with the method using RF clock power as CD monitoring signal, PMD effect is eliminated and better measurement resolution is achieved. Residual CD can also be measured through amplitude ratio in delay-tap sampling plot. By using the cost effective low bandwidth balanced receiver, the CD monitoring scheme has large CD measurement range (0~130-ps/nm) in 50% RZ DQPSK system.

ACKNOWLEDGEMENT

The authors would like to thank the supports of Singapore MOE's AcRF Tier 1 Grant R-263-000-631-112, and the help of Linghao Cheng, Zhaohui Li, Yangfu Yang, Chao Lu, Alan Pak Tao Lau, Hwa-yaw Tam and P. K. A. Wai with Photonics Research Centre, The Hong Kong Polytechnic University, Hong Kong.

REFERENCES

- [1] T. E. Dimmick, G. Rossi and D. J. Blumenthal, "Optical dispersion monitoring technique using double sideband subcarriers," *IEEE Photon. Technol. Lett.*, vol. 12, 900–902 (2000).
- [2] M. N. Petersen, Z. Pan, S. Lee, S. A. Havstad and A. E. Willner, "Online chromatic dispersion monitoring and compensation using a single inband subcarrier tone," *IEEE Photon. Technol. Lett.*, vol. 14, 570–572 (2002).
- [3] Z. Pan, Q. Yu, Y. Xie, S. A. Havstad, A. E. Willner, D. S. Starodubov, and J. Feinberg, "Chromatic dispersion monitoring and automated compensation for NRZ and RZ data using clock regeneration and fading without adding signaling," *Proc. Opt. Fiber Commun./ Nat. Fiber Opt. Eng. Conf. (OFC/NFOEC)*, WH5-1(2001).

- [4] K.-T. Tsai and W. I. Way, "Chromatic-dispersion monitoring using an optical delay-and-add filter," *J. Lightwave Technol.*, vol. 23, 3737-47 (2005).
- [5] N. Liu, W. D. Zhong, Y. J. Wen, C. Lu, L. Cheng, and Y. Wang, "PMD and chirp effects suppression in RF tone-based chromatic dispersion monitoring," *IEEE Photon. Technol. Lett.*, vol. 18, 673-675, (2006).
- [6] R. A. Skoog, T. C. Banwell, J.W. Gannett, S. F. Habiby, M. Pang, M. E. Rauch, and P. Toliver, "Automatic identification of impairments using support vector machine pattern classification on eye diagrams," *IEEE Photon. Technol. Lett.*, vol. 18, 2398-2400 (2006).
- [7] N. Hanik, A. Gladisch, C. Caspar, and B. strebel, "Application of amplitude histograms to monitor performance of optical channels," *Electronics Letters*, vol. 35, pp. 403-404 (1999).
- [8] N. Kikuchi, S. Hayase, K. Sekine, and S. Sasaki, "Performance of chromatic dispersion monitoring using statistical moments of asynchronously sampled waveform histograms," *IEEE Photon. Technol. Lett.*, vol. 17, 1103-1105 (2005).
- [9] Z. Li and G. Li, "In-line performance monitoring for RZ-DPSK signals using asynchronous amplitude histogram evaluation," *IEEE Photon. Technol. Lett.*, vol. 18, 472-474 (2006).
- [10] S. D. Dods and T. B. Anderson, "Optical performance monitoring technique using delay tap asynchronous waveform sampling," *Proc. Opt. Fiber Commun./ Nat. Fiber Opt. Eng. Conf. (OFC/NFOEC)*, OThP5, Anaheim, CA (2006).
- [11] T. B. Anderson, A. Kowalczyk, K. Clarke, S. D. Dods, D. Hewitt, and J. C. Li, "Multi impairment monitoring for optical networks," *J. Lightwave Technol.*, vol. 27, 3729-3736 (2009).
- [12] J. Zhao, Z. Li, D. Liu, L. Cheng, C. Lu, and H. Y. Tam, "NRZ-DPSK and RZ-DPSK signals signed chromatic dispersion monitoring using asynchronous delay-tap sampling," *J. Lightwave Technol.*, vol. 27, 5295-5301 (2009).
- [13] Z. Li, J. Zhao, L. Cheng, Y. Yang, C. Lu, A. P. T. Lau, C. Yu, H. Y. Tam and P. K. A. Wai, "Signed chromatic dispersion monitoring of 100Gbit/s CS-RZ DQPSK signal by evaluating the asymmetry ratio of delay tap sampling," *Optics Express*, vol. 18, 3149-3157 (2010).
- [14] B. W. Hakki, "Polarization mode dispersion compensation by phase diversity detection," *IEEE Photon. Technol. Lett.*, vol. 9, 121-123 (1997).
- [15] F. Roy, C. Francia, F. Bruyere, and D. Penninckx, "A simple dynamic polarization mode dispersion compensator," *Proc. Opt. Fiber Commun./ Nat. Fiber Opt. Eng. Conf.(OFC/NFOEC)*, 275-278, vol. 1 (1999).
- [16] N. Kikuchi, "Analysis of signal degree of polarization degradation used as control signal for optical polarization mode dispersion compensation," *IEEE/OSA J. Lightw. Technol.*, vol. 19, 480-486 (2001).
- [17] S. M. R. M. Nezam, Y. W. Song, C. Yu, J. E. McGeehan, A. B. Sahin, and A. E. Willner, "First-order PMD monitoring for NRZ data using RF clock regeneration techniques," *J. Lightwave Technol.*, vol. 22, 1086-1093 (2004).
- [18] C. Yu, Y. Wang, T. Luo, Z. Pan, S.M.R. Motaghian Nezam, A. B. sahin, and A. E. Willner, "Chromatic-dispersion-insensitive PMD monitoring for NRZ data based on clock power measurement using a narrowband FBG notch filter," *Proc. European Conference on Optical Communications Proceedings (ECOC)*, Tu4.2.3, 1-2 (2003).
- [19] F. Buchali, W. Baumert, H. Bulow, J. Poirrier, "A 40 Gb/s eye monitor and its application to adaptive PMD compensation," *Opt. Fiber Commun./ Nat. Fiber Opt. Eng. Conf.(OFC/NFOEC)*, 202-203, vol. 1 (2002).
- [20] T. B. Anderson, A. Kowalczyk, K. Clarke, S. D. Dods, D. Hewitt, and J. C. Li, "Multi impairment monitoring for optical networks," *J. Lightwave Technol.*, vol. 27, 3729-26 (2009).
- [21] J. Yang, K. Chee, and C. Yu, "CD Insensitive PMD Monitoring for Different Modulation Formats Based on RF Tone Power Measurement Using an FBG Notch Filter," *7th International Conference on Information, Communications and Signal Processing (ICICS) '09* (2009).
- [22] J. Yang, C. Yu, L. Cheng, Z. Li, C. Lu, A. P. T. Lau, H. Y. Tam, and P. K. A. Wai, "CD insensitive PMD monitoring by using FBG notch filter in 57-Gbit/s D8PSK and 38-Gbit/s DQPSK systems," *Conference on Lasers and Electro-Optics (CLEO) '10*, Paper CFC1 (2010).
- [23] J. Yang, C. Yu, L. Cheng, Z. Li, C. Lu, A. P. T. Lau, H. Y. Tam, and P. K. A. Wai, "CD insensitive PMD monitoring with large measurement range in 57-Gbit/s D8PSK and 38-Gbit/s DQPSK systems," *Optics Express*, vol. 19, no. 2, pp. 1354-1359 (2011).
- [24] J. Yang, C. Yu, L. Cheng, Z. Li, and C. Lu, "PMD insensitive CD monitoring based on RF power ratio in D8PSK and DQPSK systems," *9th International Conference on Optical Internet (COIN) '10*, Paper TuC3-3 (2010).
- [25] J. Yang, C. Yu, Y. Yang, L. Cheng, Z. Li, C. Lu, A. P. T. Lau, H. Y. Tam, and P. K. A. Wai, "PMD-insensitive CD monitoring based on RF clock power ratio measurement with optical notch filter," *accepted by IEEE Photon. Technol. Lett.*